Irregular Quad-Mode Antenna Array: Field-of-View Comparison with the Swedish LOFAR Station

Irregular Quad-Mode Antenna Array: Field-of-View Comparison with the Swedish LOFAR Station

D.S. Prinsloo[1], P. Meyer[2], R. Maaskant[3], M.V. Ivashina[4]
[1]Dept. of Electrical and Electronic Engineering, Stellenbosch University, Stellenbosch, South-Africa, 16238087@sun.ac.za
[2]Dept. of Electrical and Electronic Engineering, Stellenbosch University, Stellenbosch, South-Africa, pmeyer@sun.ac.za
[3]Dept. of Signals and Systems, Chalmers University of Technology, Gothenburg, Sweden, rob.maaskant@chalmers.se
[4]Dept. of Signals and Systems, Chalmers University of Technology, Gothenburg, Sweden, marianna.ivashina@chalmers.se

***Abstract*—The response of a 96 element quad-mode antenna (QMA) array configured in the layout of a Low Frequency Array (LOFAR) Low Band Antenna (LBA) station is assessed. Mutual coupling between the four fundamental excitation modes of each QMA is investigated and the maximum gain achieved by the QMA array is compared with the maximum gain of the LBA array. It is shown that the QMA array results in a 5 dB increase in gain toward the horizon with a variation in gain less than 5 dB over a hemispherical Field-of-View (FoV) coverage.**

***Index Terms*—antenna arrays, radio astronomy, receiving antennas.**

I. Introduction

Until recently the Very High Frequency (VHF) band has remained largely underutilized by radio astronomy receivers [1]. Following the advances in digital signal processing hardware a number of radio telescopes have been developed in the past decade to observe at meter to decameter wavelengths. These telescopes consist of large phased antenna arrays implementing electrically small antennas with broad beam patterns that allow for a large Field-of-View (FoV) coverage over which the array beam can be steered electronically. At present the largest of these phased array radio telescopes is the Low Frequency Array (LOFAR) [2] designed to operate in the frequency band ranging from 10 MHz to 240 MHz. The LOFAR telescope currently consists of 48 stations each containing two distinct arrays comprising of 96 dual-polarized antenna elements: an irregular array of inverted-V dipoles – referred to as Low Band Antennas (LBAs) – operating from 10 MHz to 90 MHz, and a more dense array of High Band Antennas (HBAs) operating from 110 MHz to 240 MHz.

In an attempt to realize a phased array antenna element that allows for near-hemispherical FoV coverage in sparse configurations, the authors recently developed a Quad-Mode Antenna (QMA) element [3], [4] that allows for four orthogonal excitation modes through which two perpendicular dipoles and an integrated monopole element can be excited. This paper investigates the response of an irregular, sparse array of QMAs by comparing the performance of the QMA array to that of one of the LOFAR LBA stations based at Onsala Space Observatory in Sweden. The QMA design is discussed in Sec. II and the performance of an isolated QMA is compared to that of the LOFAR LBA element. Section III introduces the Onsala LBA array configuration and investigates the mutual coupling between the four excitation modes of the QMA within the array environment. In Sec. IV the maximum gain realized by the QMA array, over a hemispherical FoV, is compared with that of the LOFAR LBA array. The results presented in Sec. IV illustrate that the QMA achieves a gain variation of only 5 dB over the hemispherical FoV with a 5 dB increase in gain toward the horizon when compared with the LBA array.

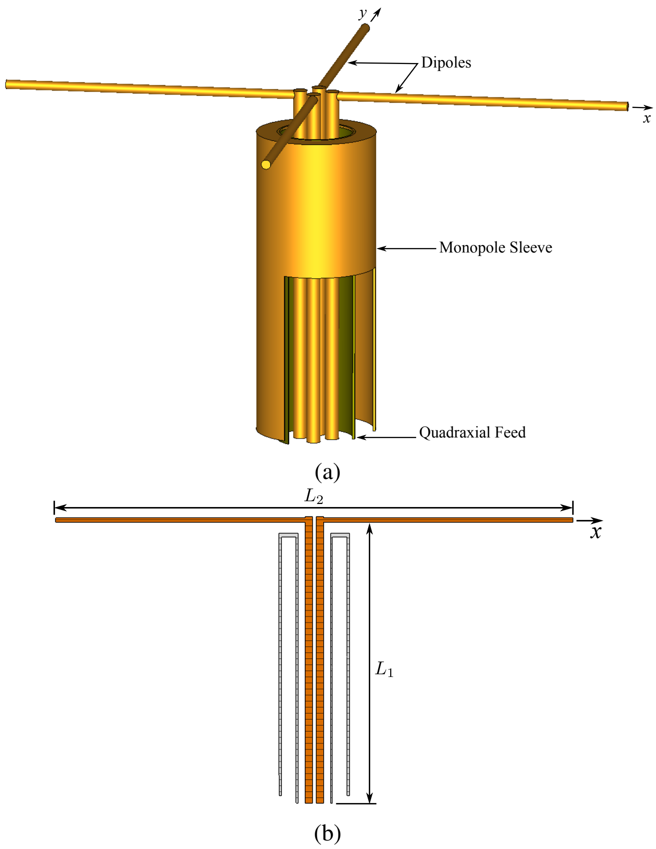

Fig. 1. Simulated quad-mode antenna design (a) sectional cut showing quadraxial feed and integrated monopole sleeve (b) y-axis normal to cut-plane [$L_1 = 1.3$ m, $L_2 = 2.52$ m].

II. Isolated Quad-Mode Antenna Response

A graphic illustration of the QMA implemented in the presented analysis is shown in Fig. 1. The design is similar to the QMA introduced in [3] but with the dimensions scaled in such a way that a resonant frequency of 55 MHz is achieved. As shown in Fig. 1(a) and (b), the QMA integrates and co-locates two horizontally oriented, perpendicular dipole elements, with a vertical monopole, all excited through a single quadraxial transmission line. The field distributions of the four fundamental Transverse Electromagnetic (TEM) excitation modes supported by the quadraxial feed, TEM_1 – TEM_4, are shown in Fig. 2(a)–(d), with the radiation patterns corresponding to each excitation mode depicted in Fig. 2(e)–(h).

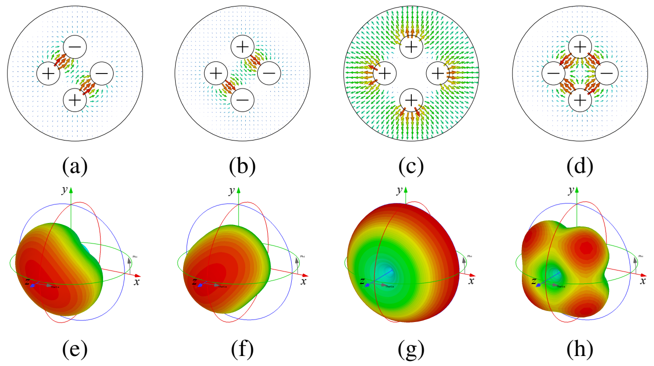

Fig. 2. Field distribution of port excitation modes (a) TEM_1 (b) TEM_2 (c) TEM_3 (d) TEM_4, with corresponding far-field radiation patterns for (e) TEM_1 (f) TEM_2 (g) TEM_3 (h) TEM_4.

Excitation modes TEM_1 and TEM_2 excite the arms of each dipole differentially and result in typical dipole-over-ground radiation patterns. Mode TEM_3 is seen to excite the four inner conductors in-phase and causes the QMA to radiate in a monopole fashion [c.f. Fig. 2(g)]. The fourth excitation mode excites each adjacent dipole arm out-of-phase, resulting in power radiated diagonally with respect to the orientation of the dipole arms.

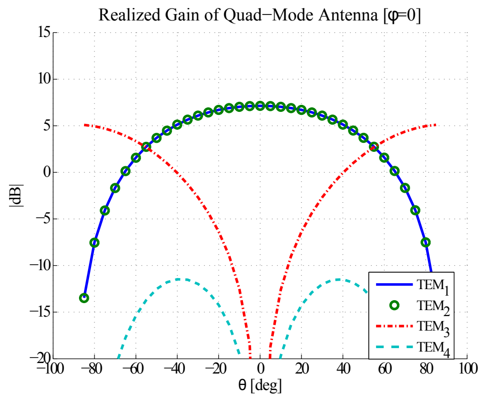

Fig. 3. Realized gain of QMA.

The graph in Fig. 3 shows the realized gain of each excitation mode in the $\phi = 0°$ plane — as simulated at 55 MHz over an infinite ground plane in CST. It is clear that through the effective utilization of the available excitation modes, near hemispherical FoV coverage can be achieved.

Solving complex beamforming weights for each excitation mode $\mathbf{w} = [w_1 \ldots w_N]^T$ through conjugate field matching [5], the gain of the QMA can be maximized at each scan angle $\Omega = (\theta, \phi)$. The weighted gain $(G(\Omega))$ of the QMA is then be obtained from

$$G(\Omega) = \frac{2\pi}{\eta} \left[\frac{\left| \sum_{m=1}^{N} w_m \boldsymbol{f}_m(\Omega) \right|^2}{\mathbf{w}^H \left[\mathbf{I} - \mathbf{S}^H \mathbf{S} \right] \mathbf{w}} \right] \quad \text{for } N = 4 \qquad (1)$$

with η denoting the free-space impedance, $\boldsymbol{f}_m(\Omega)$ the embedded radiation pattern of the antenna for excitation mode TEM_m, $\mathbf{I}$ an $[N \times N]$ identity matrix, $\mathbf{S}$ the $[N \times N]$ S-matrix of the QMA, and the superscript ^{H} the conjugate transpose.

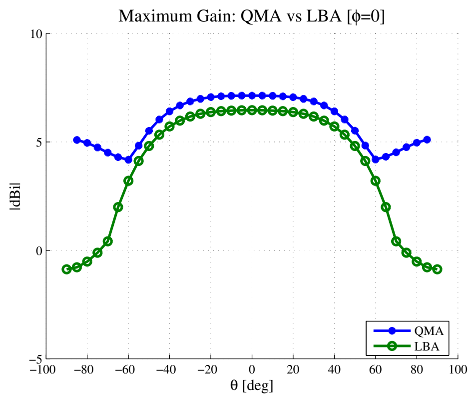

Fig. 4. Comparison of LBA and maximized QMA gain patterns.

In Fig. 4 the maximum gain of the QMA is compared with the maximum gain achieved by the LOFAR LBA element, simulated over an infinite ground plane at 55 MHz, in the $\phi = 0°$ plane. It is seen that the QMA realizes a variation in gain of less than 3 dB over the scan range from $-90°$ to $90°$, whereas the gain achieved by the LBA element reduces by nearly 7 dB over the same scan range.

III. Mutual Coupling of Quad-Mode Antenna Array

The array configuration of the 96 element LBA station at Onsala is shown in Fig. 5. Using the integral-equation-based solver CAESAR [6], both the LBA and QMA arrays are simulated at 55 MHz in the configuration shown in Fig. 5 with an infinite ground plane. Through the use of the simulated S-matrix of the 96 element QMA array the mutual coupling present in the array environment between the respective excitation modes can be assessed. Figures 6(a)–(d) depict the magnitude of the S-parameters corresponding to excitation modes TEM_1 – TEM_4 of each array element, respectively.

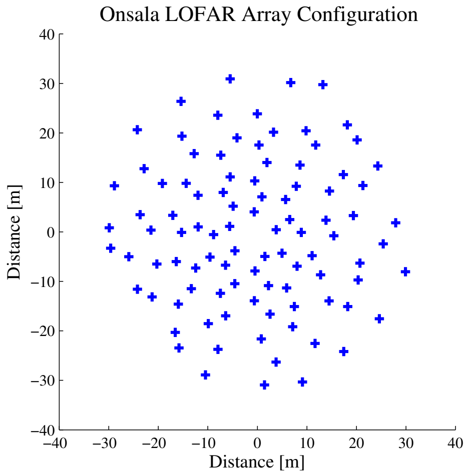

Fig. 5. Onsala LOFAR LBA array configuration.

From Figs. 6(a)–(d), the input reflection coefficients – shown along the diagonal of each graph – are seen to be below -10 dB for modes TEM_1 – TEM_3, with mode TEM_4 largely mismatched. Given the low radiated power of mode TEM_4, mutual coupling between the elements of the array is below -30 dB when excited with mode TEM_4 [c.f. Fig. 6(d)]. Due to the similar radiation characteristics of modes TEM_1 and TEM_2 the mutual coupling between the QMA elements [c.f. Fig. 6(a) and (b)] are seen to be nearly identical for these two excitation modes. Since the QMA radiates in a dipole-over-ground fashion when excited by modes TEM_1 and TEM_2, little power is radiated toward adjacent array elements, resulting in low mutual coupling between the elements. As shown in Fig. 6(c), the monopole-like radiation pattern of mode TEM_3 results in significantly more mutual coupling between the array elements. Despite the relatively close proximity of some of the array elements, mutual coupling between the elements remain below -15 dB for all excitation modes. Given the orthogonal nature of the four excitation modes, the simulated cross-coupling between modes are below -20 dB and are therefore omitted.

IV. Maximum Gain of Quad-Mode Antenna Array

Using (1) the gain of the QMA array can be computed over the hemispherical FoV, where $N = 384$ for the four excitation modes of the 96 element array. Once again conjugate field matching is applied to solve the weight set $\mathbf{w} = [w_1 \ldots w_{\mathrm{N}}]^T$ in order to maximize the QMA array gain at each scan angle Ω. The graphs in Fig. 7(a) and (b) show the maximum gain achieved by the QMA and LBA arrays over the hemispherical FoV.

The QMA array [c.f. Fig. 7(a)] achieves slightly higher gain at boresight compared to the LBA array [c.f. Fig. 7(b)], with the variation in gain of the QMA array below 5 dB over the hemispherical FoV coverage. The LBA array, in comparison, shows a reduction in gain of approximately 8 dB when scanning toward the horizon. Comparing the variation in gain of the

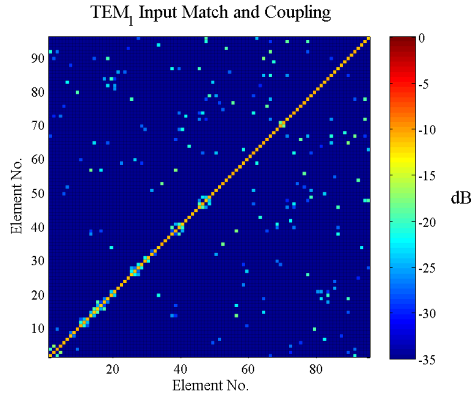

(a)

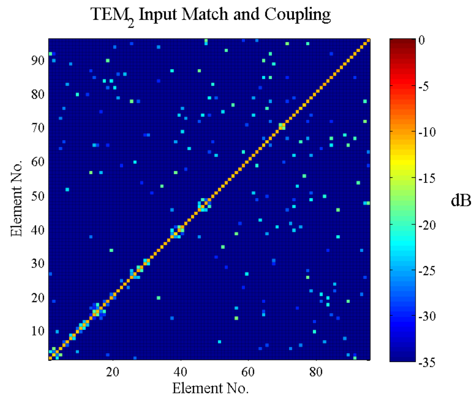

(b)

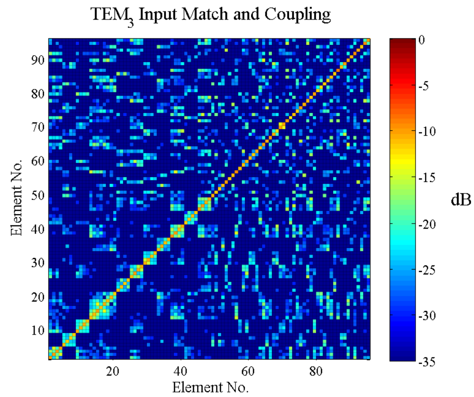

(c)

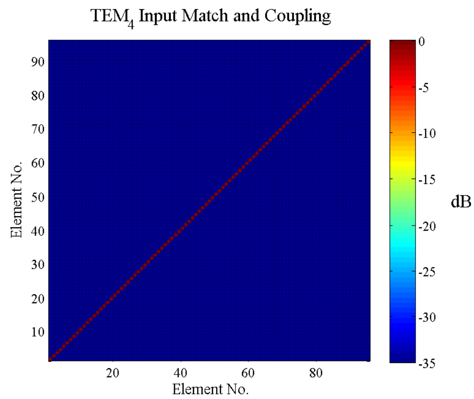

(d)

Fig. 6. Magnitude of the S-paramters of each TEM excitation mode of the QMA array.

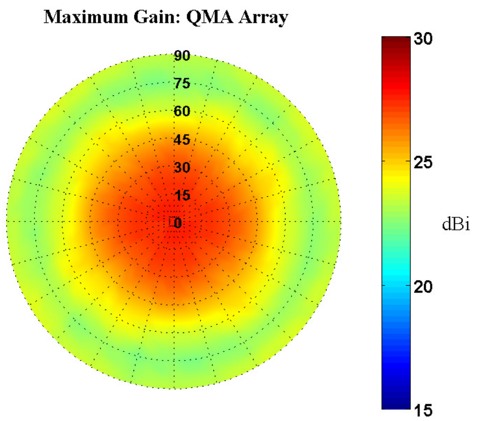

(a)

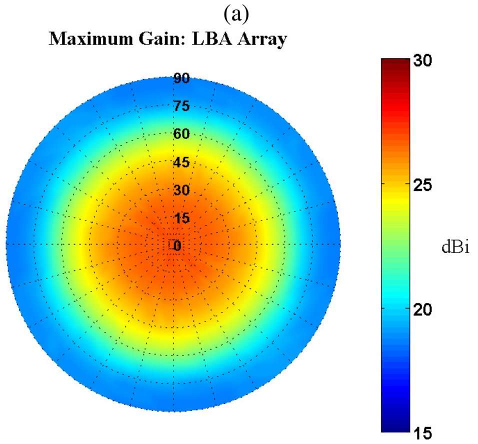

(b)

Fig. 7. Maximum gain over the hemispherical FoV (a) QMA array, and (b) LBA array.

QMA array to that of the single isolated element [c.f. Fig. 4] a 2 dB increase in gain variation is observed for the QMA array. To gain a better understanding of this increased variation in gain observed for the QMA array, the response of an array of hemispherically radiating point source elements positioned in the LBA array configuration is assessed. The fields radiated by each point source element $\boldsymbol{E}_{\mathrm{m}}^{\mathrm{p}}(\theta, \phi)$ $(\mathrm{m} = 1, ..., 96)$, is defined in the Ludwig-3 coordinate system [7] as

$$\boldsymbol{E}_{\mathrm{m}}^{\mathrm{p}}(\theta, \phi) = \begin{cases} [1\hat{\boldsymbol{a}_{\mathrm{CO}}} + 1\hat{\boldsymbol{a}_{\mathrm{XP}}}]\, e^{jk\hat{\boldsymbol{r}}\cdot\boldsymbol{r}_{\mathrm{m}}} & \text{for } |\theta| < 90^{\circ} \\ 0 & \text{for } |\theta| \geq 90^{\circ} \end{cases} \quad \forall\, \phi \tag{2}$$

where k denotes the wave number, the vector $\boldsymbol{r}_{\mathrm{m}}$ is directed toward the m^{th} point source element in the the array configuration [c.f. Fig. 5], and $\hat{\boldsymbol{r}}$ is a unit vector directed toward the point of observation. Since the point source elements are ideal, no deformation of the embedded elements patterns occur within the array environment and the resulting gain of each element is therefore 3 dBi over the entire hemispherical FoV.

In Fig. 8 the maximum gain over the scan range from -90° to 90° of the QMA, LBA, and point source arrays are compared in the $\phi = 0^{\circ}$ plane, where a similar 2 dB variation in the gain of the array of point source elements is observed. The reduction in gain at larger scan angles can

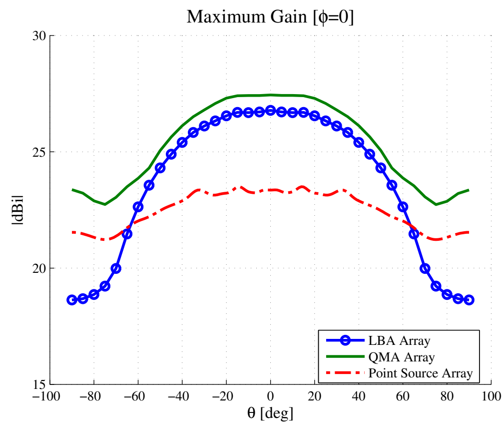

Fig. 8. Comparison of the maximized gain of the QMA and LBA arrays with an array of hemispherically radiating point source elements.

therefore largely be ascribed to the phase variation of the embedded element patterns due to the geometry of the array as opposed to shielding and mutual coupling of the physical antenna elements within the array.

V. Conclusion

Using the layout of the LOFAR LBA station at Onsala space observatory in Sweden, the maximum gain of a QMA array has been compared with the maximum gain achieved by the LBA array over a hemispherical FoV. It is shown that the mutual coupling between the four fundamental excitation modes of the QMA elements are below -15 dB, with the monopole-like radiation pattern of excitation mode TEM_3 resulting in the largest coupling between the QMA elements. The QMA array shows a 2 dB increase in gain variation over the FoV coverage compared with that of a single isolated QMA. Through the simulated response of an identical array of hemispherically radiating point source elements it is illustrated that the dominant cause of the reduction in gain observed at larger scan angles is due to destructive field interference caused by the element spacing within the array. Despite the increased gain variation, the QMA array still exhibits a 5 dB increase in gain towards the horizon when compared with the LBA array. Since the layout of the LBA station has not been optimized for the QMA array, future work will be done toward an optimized QMA array configuration wherein the sensitivity and polarimetric response of the QMA array will be assessed.

Acknowledgment

This research was supported by a MCA International Research Staff Exchange Scheme Fellowship within the European FP7 Programme, contract no. 612599. The authors would also like to acknowledge SKA SA, the South African Research Chairs Initiative of the DST, the NRF, as well as the Swedish VR and VINNOVA agencies for funding this work.

References

[1] M. Garrett, "Radio astronomy transformed: Aperture arrays; past, present and future," in *AFRICON*, Sept 2013, pp. 1–5.

[2] M. van Haarlem *et al.*, "LOFAR: The low-frequency array," *Astronomy and Astrophysics*, vol. 556, Aug. 2013.

[3] D. Prinsloo, P. Meyer, M. Ivashina, and R. Maaskant, "A quad-mode antenna for accurate polarimetric measurements over an ultra-wide field-of-view," in *8th European Conf. on Antennas and Propag. (EuCAP)*, April 2014, pp. 3794–3797.

[4] D. Prinsloo, R. Maaskant, M. Ivashina, and P. Meyer, "Mixed-mode sensitivity analysis of a combined differential and common mode active receiving antenna providing near-hemispherical field-of-view coverage," *IEEE Trans. Antennas Propag.*, vol. 62, no. 8, pp. 3951–3961, Aug. 2014.

[5] M. Ivashina *et al.*, "An optimal beamforming strategy for wide-field surveys with phased-array-fed reflector antennas," *IEEE Trans. Antennas Propag.*, vol. 59, no. 6, pp. 1864–1875, June 2011.

[6] R. Maaskant, R. Mittra, and A. G. Tijhuis, "Fast analysis of large antenna arrays using the characteristic basis function method and the adaptive cross approximation algorithm," *IEEE Trans. Antennas Propag.*, vol. 56, no. 11, pp. 3440–3451, Nov. 2008.

[7] A. Ludwig, "The definition of cross polarization," *IEEE Trans. Antennas Propag.*, vol. AP-21, no. 1, pp. 116–119, Jan. 1973.